journal

J. Am. Ceram. Soc., 74 [8] 1922–27 (1991)

Acoustic Emission During Micro- and Macrocrack Growth in Mg-PSZ

A.V. Drozdov, Velodya O. Galenko, and George A. Gogotsi

Institute for Problems of Strength, Ukranian Academy of Sciences, Kiev-14, USSR

Michael V. Swain*

Department of Mechanical Engineering, Advanced Materials Technology Centre, The University of Sydney, New South Wales 2006, Australia

Acoustic emission (AE) of a Mg-PSZ (TS grade) material has been studied during three- and four-point bending and stable macrocrack extension tests. During flexure, AE signals increased significantly upon the onset of nonlinear stress–strain behavior and were associated with phase transformation and microcracking on the tensile surface. Observations of crack extension in notched bars revealed relatively little AE during initial loading and onset of nonlinear behavior. However, on subsequent loadings, the number of counts was in reasonable agreement with the extent of crack growth. These observations are discussed in terms of AE from phase transformation and crack growth at different grain size. They are compared with AE behavior of other zirconia-based materials. [Key words: acoustic emissions, crack growth, magnesia, zirconia-partially stabilized (PSZ), *R*-curve.]

I. Introduction

FRACTURE mechanics studies of transformation-toughened ceramics have led to considerable differences in the nominal toughness of these materials when evaluated using different techniques. While it is difficult to generalize as to the reliability of the different techniques, as a general observation it may be said that approaches that generate equilibrium crack growth prior to unstable or quasi-stable failure are more valid. In addition the *R*-curve phenomenon in most transformation-toughened ceramics leads to a nonunique estimation of K_{Ic} but requires in some instances many millimeters of crack extension before attaining a steady-state value.

One technique that is suitable for the monitoring of crack extension in a qualitative manner is acoustic emission (AE). With this method small bursts of energy involved in the rupturing events at the crack tip are detected by a very sensitive piezo transducer and preamp system. Previous studies by Linzer and Evans[1] have attested to the ability of AE to monitor slow crack growth in a range of polycrystalline materials but not for fully dense homogeneous isotropic materials such as glasses. Acoustic emission has been utilized by a few authors to monitor behavior in zirconia transforming materials. Clarke and Arora[2] used AE to monitor the transformation of pure zirconia powders that had been sintered at 1500°C, then slowly cooled through the tetragonal-to-monoclinic (*t*- to *m*-ZrO_2) phase transformation and to ambient temperature. Acoustic emission events were considered to emanate from both the phase transformation and associated cracking of the material, which was both macro- and microcrack growth. In comparison, the behavior of unstabilized zirconia exhibited AE events only between 1250° and 900°C associated with the phase transformation.

Lankford[3] used AE to monitor the deformation and failure of Mg-PSZ materials during compressive loading. He observed that AE events occurred only well after the onset of yielding and were associated with the serrated region of the work-hardening curve prior to failure. At higher temperature (700°C), at which the onset of yielding did not occur, AE events took place only upon failure. These observations by Lankford[3] led him to conclude that AE during loading was associated only with microfracturing and not the *t*- to *m*-ZrO_2 transformation.

In this paper the aims are to compare the AE signals emanating from a simple loaded beam in flexure with and without a notch from which to initiate stable crack growth. Previous studies have shown that, for TS grade material, stable crack growth will occur in both instances.[4] For a deep notch, stable crack extension and a rising *R*-curve over 1 mm of crack growth were observed, whereas, for a beam in flexure, previous results have also established that small cracks are initiated at grain boundaries and grow in a stable manner before catastrophic failure of the beam occurs. AE data generated from both types of tests are studied, and the application of the former to generate a *K–V* curve are given.

II. Experimental Procedures

(1) Material

The material evaluated in this study was a commercially available TS grade Mg-PSZ sample obtained from Nilcra.* Previous data obtained with the same material were reported on by Veitch *et al.*[5] Samples were prepared by diamond grinding to the requisite size prior to testing. The single-edge-notched bend (SENB) sample was prepared by notching to approximately half the thickness with a 0.15 mm wide diamond saw. For comparison, the AE data for two Soviet Y-PSZ materials are included.[6] These materials and properties are compared in Table I.

(2) Flexure Tests

Flexure tests were conducted with the aid of a purposely built four-point-bending rig[7] that enabled load and displacement to be simultaneously monitored. The displacement was monitored by a precision linear variable differential transformer with a resolution of ~0.1 μm. Specimens tested were 3.5 mm × 5 mm × 50 mm and had beveled edges. The

A.V. Virkar—contributing editor

Manuscript No. 197428. Received July 30, 1990; approved March 26, 1991.
Supported by Nilcra Ceramics, Clayton, Victoria, Australia; and the Australian Department of Industry, Technology and Commerce.

*Member, American Ceramic Society.

*Nilcra Ceramics, Clayton, Victoria, Australia.

Table I. Properties of Y-PSZ

	Contents of Y_2O_3 (wt%)	Density (g/cm^3)	Velocity of sound (km/s)	Modulus of elasticity (GPa)		Grain size (μm)	Four-point bending MOR (MPa)	Fracture toughness ($MPa \cdot m^{1/2}$)	
				Dynamic	Static			Specimen w/notch	Specimen w/crack
6Y-PSZ	6	5.81	6.06	214	196	3	740	9.2	4.0
5Y-PSZ	5	5.80	5.98	207	191	1–3	293	4.7	2.8

strength and deflection during bending were also measured on samples annealed at 700°C for 15 min.

(3) Fracture Toughness

The fracture toughness was determined using the SENB technique with sample size 5 mm × 3.5 mm × 25 mm. Stable crack growth was achieved by the use of a stiff loading system and slow strain rate. Crack growth was monitored optically after each load–unloading sequence. Analysis was via the expression given by Strawley.[8]

(4) Acoustic Emission

The acoustic emission signal was detected with the aid of a piezo transducer connected to a preamp system with approximately 50 dB gain, and a total gain of 95 to 100 dB. The level of AE pulse amplitude discrimination is 1 V with the AE count rate determined over 0.5 s. The operating frequency range of the detector system is 100 kHz to 1 MHz.[7] The detector was mounted on the end of the rectangular flexure or SENB test bar, which acted as a wave guide for emission generated at the notch tip or tensile region of the flexure bar. An acoustic coupling grease was used to bond the detector to the test specimen. The total number of pulses N and the pulse count rate $\dot{N}$ were used as the micro- and macrocrack propagation parameters. From the total AE count, the current value of the crack length increment was determined.

$$\Delta C_m = \left[\frac{C_f - C_i}{N_f}\right] N_m \tag{1}$$

where C_i and C_f are the initial and final values of the crack length, N_f is the limiting value of the total AE counts which corresponds to the crack length C_f, and N_m is the current value of the total AE counts.

To plot the K versus V curve, the crack growth rate (derivative of the crack length increment with respect to time) was determined from the formula

$$V = \left[\frac{C_f - C_i}{N_f}\right] \dot{N} \tag{2}$$

where $\dot{N}$ is the AE count rate.

III. Observations and Discussion

Four-point-bend flexure tests on the Mg-PSZ material exhibited excellent reproducibility. In all instances the modulus of rupture was exceptionally consistent with a Weibull modulus, estimated from the samples tested, in excess of 40.[9] The other noteworthy feature was the extent of inelastic behavior in a material so strong. The load versus deflection of the center span for the material before and after annealing at 700°C for 15 min is shown in Fig. 1.

From the observations shown in Fig. 1, the average stress versus strain on the tensile surface was computed. In this case, only nonlinearity of the load–deflection curve was taken into account, while the difference in strain values on tensile and compressive surfaces of the flexure specimen was not considered. This was done using the relationships presented elsewhere, namely[10]

$$\sigma_{av} = \frac{2\alpha}{bh^2}\left(P + \frac{\delta\, dP}{2\, d\delta}\right) \tag{3}$$

$$\epsilon = \frac{4h}{L^2}\delta$$

where P is the force; δ is the deflection over the tensile span region L; and b, h, and α are the width, height, and length of the moment arm.

The stress-versus-strain curve resulting from such an analysis of the data in Fig. 1 is shown in Fig. 2. These observations show an initial linear elastic behavior followed by "yield"-like behavior with significant inelastic strain, although the extent of the inelastic strain was much higher in the annealed material (0.26%) than in the ground sample (0.18%).

These observations are comparable to flexure studies by Marshall[11] and Swain and Rose,[12] who conducted similar tests on Mg-PSZ-TS material. There is a very close agreement between the annealed stress–strain curve shown in Fig. 2 and that measured by Marshall[11] using direct tensile tests.

Over the last decade, Gogotsi[10] has suggested an alternative energetics basis for characterizing the nonlinear stress–strain behavior of materials in terms of a χ value. This term is defined by the relationship

$$\chi = \sigma_u^2/2E \int_0^{\epsilon_u} \delta_m\, d\epsilon \tag{4}$$

where σ_u is the ultimate strength, E the elastic modulus, ϵ_u the ultimate strain, and δ_m the displacement at a strain ϵ. Values of χ are readily determined from flexural load–deflection curves of a material and, as such, their measurement at elevated temperature is relatively simple. A simple schematic illustrating Eq. (4) and determination of χ is shown in Fig. 3.

Flexural tests were also conducted at elevated temperatures from 300° to 1400°C and are shown in Fig. 4. These results show a reduction in the nonlinear behavior and an initial increase in the associated χ value with increasing temperature to 600°C. At 1200°C and above, the χ value begins to decrease associated with nonlinear behavior during loading due to high-temperature creep phenomenon.

The observations in Figs. 1 and 2 highlight the significant difference in the stress–strain behavior of the ground (χ = 0.44) and annealed (χ = 0.34) specimens. Thermal expansion

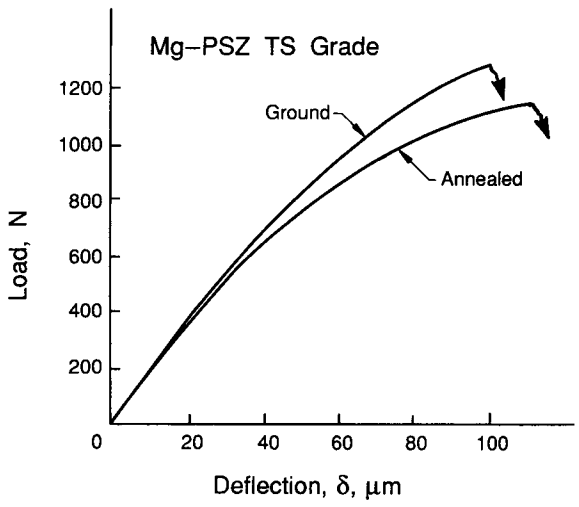

Fig. 1. Observations of the load versus deflection of the center span of four-point-loaded beams of Mg-PSZ (TS grade) before and after annealing at 700°C for 15 min.

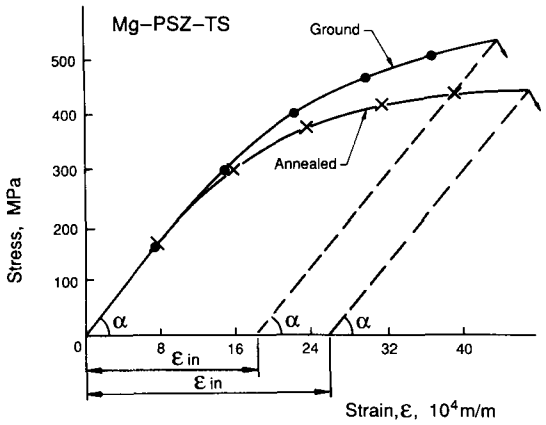

Fig. 2. Stress versus strain of Mg-PSZ (TS grade) computed from the load–deflection curves of Fig. 1 with the aid of Eq. (3), before and after annealing at 700°C for 15 min. Note the much larger residual offset for the annealed specimen. The χ parameter is defined in Eq. (4).

observations of the TS grade Mg-PSZ upon heating and cooling to 900°C are shown in Fig. 5. The data show that heating this material to 700°C exceeds the reverse monoclinic-to-tetragonal phase transformation (A_s) temperature and that, upon cooling, this material retains its tetragonal phase with a measurable length reduction of 0.11%. Such a reduction in length corresponds to approximately an 8% increase in the tetragonal content. This increase in very metastable tetragonal phase is responsible for the greatly enhanced ductility and observed 30% increase in the strain to failure (ϵ_f).

The flexure tests were observed to produce considerable AE signals, which began almost immediately upon loading and significantly increased the rate upon subsequent loading. Observations of the contact sites after fracture revealed significant damage in the form of transformation and microcracking. The extent of signal generation was reduced when 0.3-mm sheets of poly(vinyl chloride) (PVC) were placed between the metallic rollers of the flexure rig and the specimen. Examples of the signal generation during testing after inserting the polymeric sheets between the sample and loading fixture are shown in Fig. 6 for two crosshead rates. At the slower stressing rate, considerable AE signal generation occurred just prior to failure, suggesting that significant stable microcrack growth occurred accompanying the transformation of the tetragonal phase.

Previous studies by Swain,[4] Marshall,[11] and Marshall and Swain[13] have observed and considered the initiation and ex-

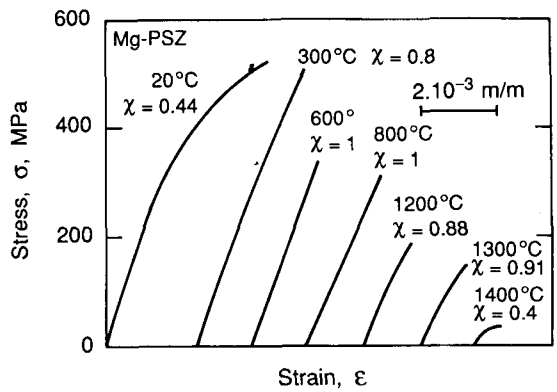

Fig. 3. Stress–strain curves for Mg-PSZ at different temperatures computed from load versus center span deflection curves as illustrated in Figs. 1 and 2. Note that the brittleness index χ increases with increasing temperature up to 800°C as the transformation ductility decreases, whereas at 1200°C and above the value of χ decreases because of creep-related ductility.

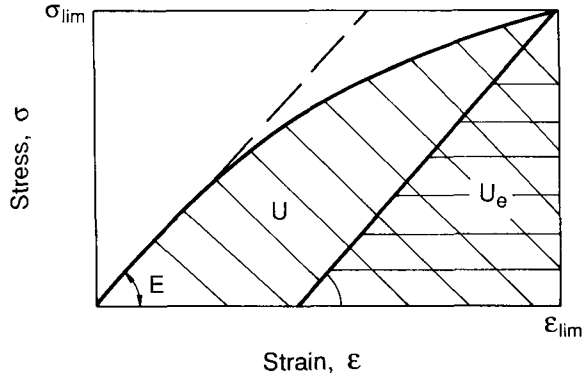

Fig. 4. Schematic illustration of the stress–strain curve of a nonlinear-behaving material. The value of χ is based upon the ratio of U_e to U.

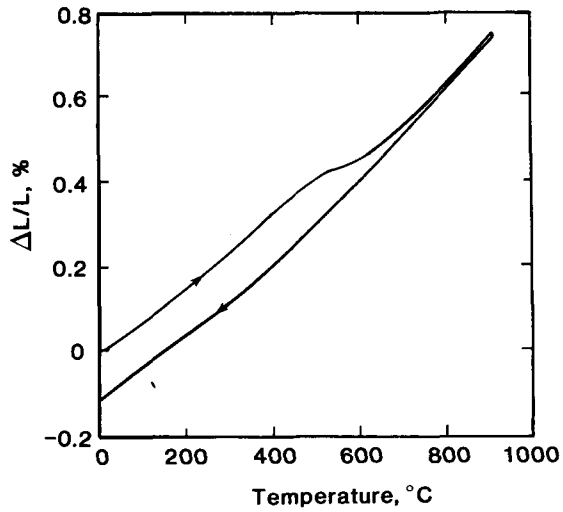

Fig. 5. Thermal expansion curve to 900°C of Mg-PSZ (TS grade) upon heating and cooling. The residual contraction is indicative that some of the monoclinic zirconia has retained the tetragonal form upon cooling.

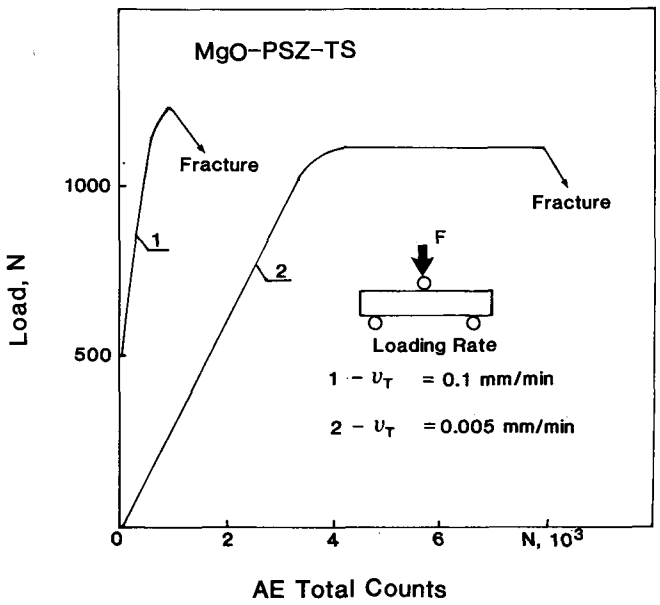

Fig. 6. Acoustic emission events during three-point loading of Mg-PSZ at two different crosshead speeds. The larger number of events at the slower loading rate suggests more microcracking occurs and that environmental effects are important.

tension of microcracks on the tensile surface of flexure bars of TS grade material. Examples of these cracks are shown in Fig. 7. Monitoring the growth of such flaws enables an R-curve to be constructed for such materials. In many instances the initiation of such cracks as shown in Fig. 7 occurs from pores along grain boundaries. Recently Marshall and Swain[14] have proposed that the observed rumpling of PSZ surfaces under stress is due to the known elastic anisotropy of cubic zirconia, and this feature is most pronounced for constrained grains of differing orientations at the surface. The presence of a pore at a grain boundary subjected to remote tension and where such elastic anisotropy stresses are tensile would provide a stress concentration site for grain-boundary cracking and/or localized tetragonal-to-monoclinic phase transformation.

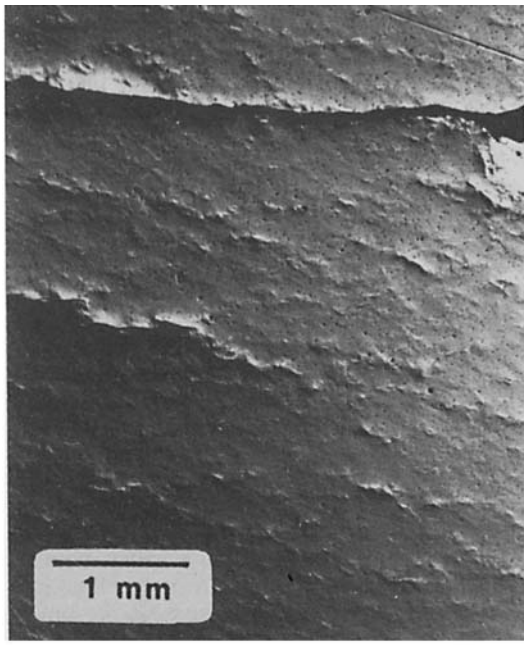

(A)

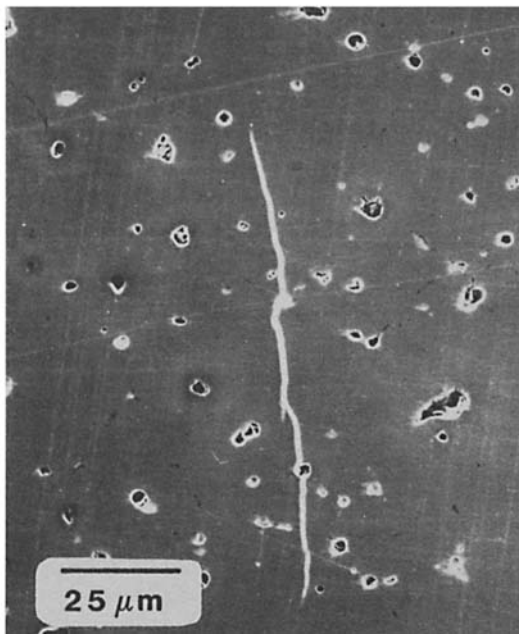

(B)

Fig. 7. (A) Optical and (B) scanning electron micrographs of cracks that develop on the tensile surface of beams in flexure. The optical observations are aided by surface uplift accompanying the tetragonal-to-monoclinic phase transformation about the crack tip and by use of the Normaski interference technique. Note the initiation of cracks from a pore located in the grain boundary upon viewing the surface at high magnification in the scanning electron microscope.

Fracture toughness tests using the SENB technique lead to the load–displacement observations as shown in Fig. 8. Also shown in this figure as an insert are the total AE counts for each crack extension cycle. These observations show that the material displays the Kaiser effect; that is, upon reloading, AE signals are generated only with additional crack extension. There is a small amount of AE activity on the unloading cycle. The load deflection observations are essentially identical to those previously reported by Swain and Hannink;[15] they display small hysteresis loops and significant nonlinearity upon unloading due to transformation-related crack face closure effects. The crack length after each cycle was measured optically with a traveling microscope so as not to rely on the compliance relationship.

The number of AE events as a function of crack length has been measured for an initiating crack and a well-developed crack ~1.0 mm long. These results are shown in Fig. 9. The Mg-PSZ material initially shows increasing AE counts per unit of crack growth, whereas the Y-PSZ and a Y-TZP material remain constant (Fig. 9(A)). The steady-state crack propagation reveals that the number of AE events per unit of crack extension is least for the Mg-PSZ, intermediate for the Y-PSZ, and greatest for the Y-TZP. Such observations are the inverse of the measured K_{Ic} values of these materials; however, they are inversely related to the grain sizes. The grain size of the Mg-PSZ is ~50 μm, the Y-PSZ ~3 μm, and the Y-TZP ~1 μm. Similar observations of linear AE events per increment of crack extension but inversely related to the grain size have been reported by Knehans *et al.*[16] for a range of sintered (polygranular) glass materials. These authors argued that for fine-grained materials the fracture of a grain occurs as one major event, whereas for coarser materials it occurs as a number of partial events, although the area of material generated per event increases with increasing grain size. They were able to support such conclusions with the aid of detailed scanning electron microscopy of the fracture surfaces. For the Mg-PSZ material one may have anticipated that crack precipitate interaction would generate more AE events than for a homogeneous material such as glass; however, this is not supported by the observations in Fig. 9. Knehans *et al.*[16]

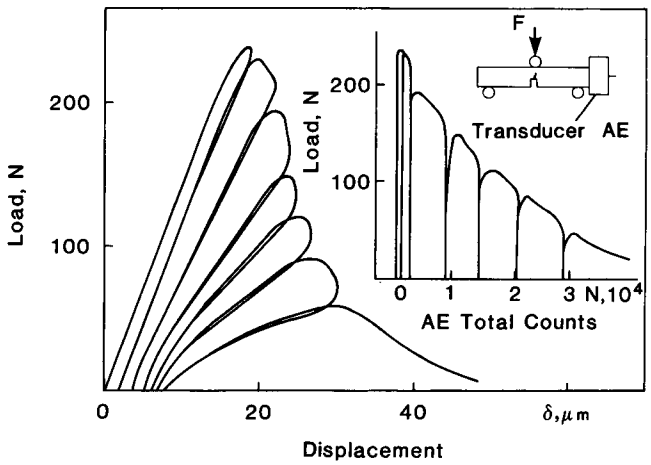

Fig. 8. Observations of the load–load point displacement curves for notched Mg-PSZ (TS grade) tested in flexure. A series of load–unloading curves after various increments of crack growth and associated compliance change are plotted. Also included as an insert are the total acoustic emission events versus load for each load–unload cycle.

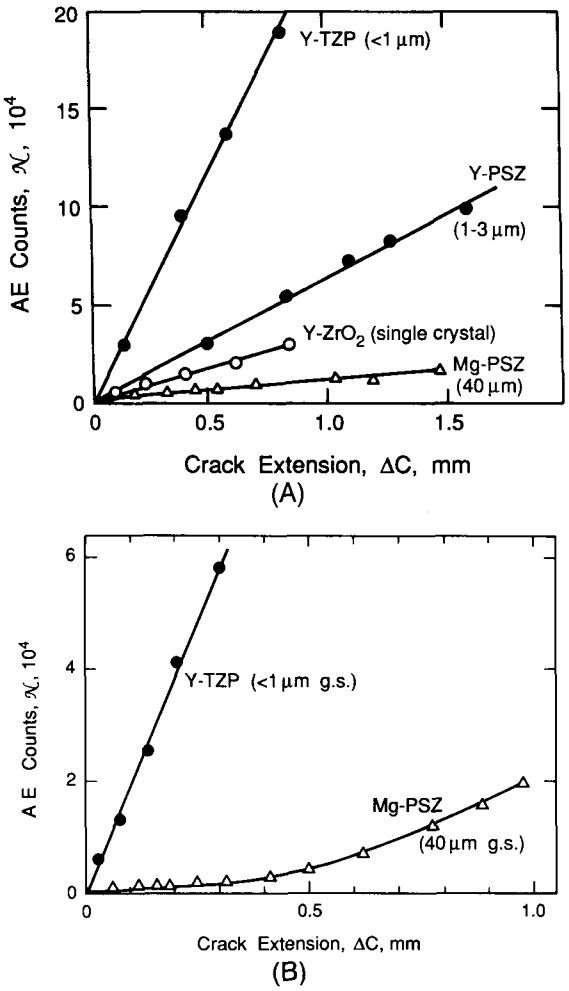

Fig. 9. (A) Acoustic emission events as a function of crack growth for four zirconia ceramics of differing grain size are shown. (B) For the Mg-PSZ and Y-TZP material, the initial stages of crack extension highlighting the increasing count per unit of crack growth are plotted.

did note that for the coarser grained materials the energy associated with each AE event was much greater than for the fine-grained materials. Although transmission electron microscopy reveals that small microcracks develop about the transformed precipitates during the passage of a crack in Mg-PSZ,[17] the energy and frequency associated with such events may exclude them from detection.

The fracture toughness (K_R) versus crack length from the direct optical and AE data shown in Fig. 8 is plotted in Fig. 10. The superimposed AE-derived R-curve was calculated from the data plotted in Fig. 9(B) from Eqs. (1) and (2), assuming near-constant crack growth rate. These observations are again similar to those of Swain and Hannink[15] and show a steeply rising R-curve with crack initiation at ~6 MPa·$m^{1/2}$ and after 1 mm of crack growth leveling off at ~12 MPa·$m^{1/2}$. For comparison, Fig. 10 shows the results of K_R curves calculation on elastically deformed Y-PSZ ceramics (χ = 1) stabilized with 5 and 6 wt% of Y_2O_3 (1- to 3-μm grain size) which displayed no K_R increase with crack length. Note that in this case the K_{Ic} values obtained by the notched bar technique (without the sharp crack) from the measured maximum load values were 9.2 and 4.7 MPa·$m^{1/2}$, respectively (Table I).

On the basis of the AE counts it is possible to determine a K–V relationship from subcritical crack growth in the stable crack growth region of a load–displacement curve. These tests were performed by stably loading the specimen such that approximately 0.5 to 1.0 mm of crack growth occurred. The crosshead of the loading machine was then stopped and the load gradually relaxed because of subcritical crack growth.[18] An example of the K–V diagram computed from the AE data is shown in Fig. 11. The possibility of determining the K–V curve from changes in the specimen compliance which can be obtained from the load–displacement curve was also evaluated. The above methods gave comparable results, but the use of the AE method which is of higher sensitivity enabled lower values of the crack growth rate to be measured. The slope of the data in Fig. 11, or n value, from the usual power law fit to this curve ($V = AK^n$) was found to be 40 to 45, much lower than results from large DCB samples, which typically give values of 90 to 100.[19] There may be two explanations for this difference; one is that the results shown in Fig. 11 were determined in the rising region of the R-curve rather than in the steady-state toughness regime as in a large DCB sample; the other possibility might be the limited range of crack velocities over which the K–V curve was computed.

IV. Conclusions

The present observations reveal that acoustic emission is a very useful means of monitoring micro- and macrocrack growth rate in zirconia ceramics. The Mg-PSZ TS grade

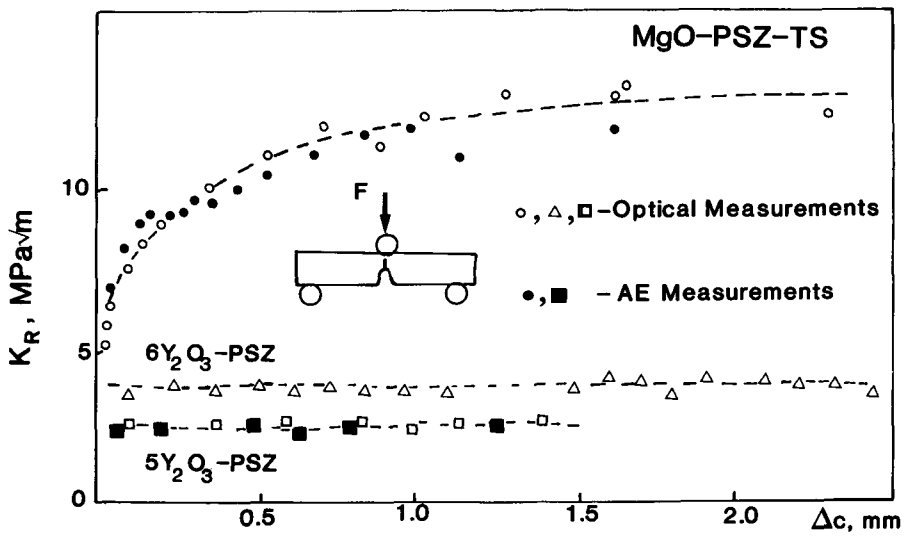

Fig. 10. R-curve of Mg-PSZ calculated from the load–deflection curves and acoustic emission data shown in Fig. 7. Also included are the K versus crack length curves for two Y-PSZ materials listed in Table I.

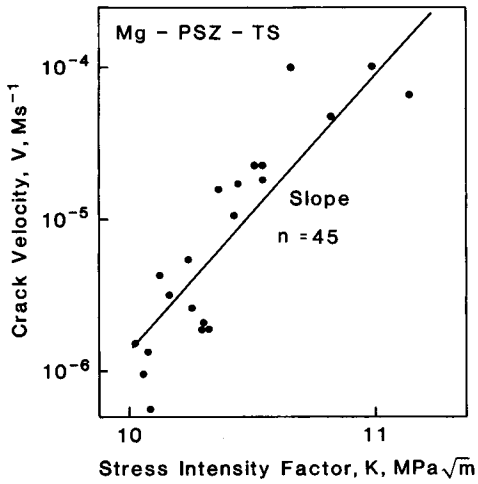

Fig. 11. Computed crack-velocity–stress-intensity factor (V–K) diagram for Mg-PSZ (TS grade) from acoustic emission data generated during a load relaxation test obtained by stopping the crosshead after ~1 mm of crack extension.

material, because of its exceptional behavior, particularly "ductility" and R-curve behavior, proved exceptionally interesting. The AE events during ductile deformation of this material appeared to be associated with microcracking on the tensile surface. This feature was most pronounced at very low stressing rates, where a considerable number of AE events were detected with minimal increase in load. Apart from the AE events, considerable increased ductility of the Mg-PSZ was observed upon annealing at 700°C. Dilatometer observations indicated that this was due to the retention of an increase of the volume content of metastable tetragonal phase upon cooling.

Crack growth studies of notched and precracked samples showed that the number of AE events per unit increment of crack growth for Mg-PSZ initially increased prior to attaining a constant rate, whereas for more brittle Y-PSZ and Y-TZP materials the behavior remained constant. This observation was due to the significant R-curve behavior of the Mg-PSZ and the virtual absence of such behavior in the other materials. From such data it was also observed that the number of AE events per increment of crack growth was least for the coarser grained Mg-PSZ and greatest for the very fine grained Y-TZP material. These observations were similar to those reported by Knehans *et al.*,[16] who studied polygrained sintered glass materials. It was also possible to use the AE technique to determine a crack-velocity–stress-intensity (V–K) diagram.

References

[1]A. G. Evans and M. Linzer, "Acoustic Emission in Brittle Materials," *Annu. Rev. Mater. Sci.*, **7**, 179 (1977).

[2]D. R. Clarke and A. Arora, "Acoustic Emission Characterization of the Tetragonal–Monoclinic Phase Transformation in Zirconia"; pp. 54–63 in Advances in Ceramics, Vol. 12, *Science and Technology of Zirconia II.* Edited by N. Claussen, A. H. Heuer, and M. Ruhle. American Ceramic Society, Columbus, OH, 1984.

[3]J. Lankford, "Plastic Deformation of Partially Stabilized Zirconia," *J. Am. Ceram. Soc.*, **66** [11] C-212–C-213 (1983).

[4]M. V. Swain, "In-Elastic Deformation of Mg-PSZ and Its Significance for Strength–Toughness Relationship of Zirconia Toughened Ceramics," *Acta Metall.*, **33**, 2083–2091 (1985).

[5]S. Veitch, M. Marmach, and M. V. Swain, "Strength and Toughness of Mg-PSZ and Y-TZP Materials at Cyrogenic Temperatures"; pp. 97–106 in Proceedings of the Materials Research Society Symposium, Vol. 78, *Advanced Structural Ceramics.* Edited by P. F. Becher, M. V. Swain, and S. Somiya. Materials Research Society, Pittsburgh, PA, 1987.

[6]G. A. Gogotsi, V. P. Zavada, A. I. Fesenko, and V. I. Galenko, "Fracture Toughness of ZrO_2–Based Ceramics" (in Russ.), *Probl. Proch.*, **8**, 124 (1989).

[7]G. A. Gogotsi and A. V. Drosdov, "Acoustic Emission in the Deformation and Failure of Corundum Refractories," *Ogneupory*, **4**, 15–19 (1986).

[8]J. E. Strawley, "Wide Range Stress Intensity Factor Expressions for ASTM E-399 Standard Fracture Toughness Specimens," *Int. J. Fract.*, **12**, 475–76 (1976).

[9]G. A. Gogotsi, M. V. Swain, and J. Davis, "Partially Stabilized Zirconia Ceramics and Their Behavior on Loading" (in Russ.), *Ogneupory*, **9** [1] 2–5 (1991).

[10]G. A. Gogotsi, "The Problem of the Classification of Low Deformation Materials Based on the Features of their Behavior Under Load," *Strength Mater. (Engl. Transl.)*, **9**, 77–83 (1977).

[11]D. B. Marshall, "Strength Characteristics of Transformation-Toughened Zirconia," *J. Am. Ceram. Soc.*, **69** [3] 173–80 (1986).

[12]M. V. Swain and L. R. F. Rose, "Strength Limitations of Transformation-Toughened Zirconia Alloys," *J. Am. Ceram. Soc.*, **69** [7] 511–18 (1986).

[13]D. B. Marshall and M. V. Swain, "Crack Resistance Curves in Magnesia-Partially-Stabilized Zirconia," *J. Am. Ceram. Soc.*, **71** [6] 399–407 (1988).

[14]D. B. Marshall and M. V. Swain, "Reversible Transformation and Elastic Anisotropy in Mg-ZrO_2," *J. Am. Ceram. Soc.*, **72** [8] 1530–32 (1989).

[15]M. V. Swain and R. H. J. Hannink. "R-Curve Behavior in Zirconia Ceramics"; pp. 225–39 in *Advances in Ceramics,* Vol. 12, *Science and Technology of Zirconia II.* Edited by N. Claussen, M. Ruhle, and A. H. Heuer. American Ceramic Society, Columbus, OH, 1984.

[16]R. Knehans, R. Steinbrech, and W. Schwaarwächter, "Quantitative Correlation of Acoustic Emission to the Brittle Fracture of Porous Sintered Glass," *Mater. Sci. Eng.*, **61**, 17–22 (1983).

[17]R. H. J. Hannink and M. V. Swain; unpublished work.

[18]G. A. Gogotsi, V. A. Kuzmenko, S. V. Grishakov, A. N. Negovski, and A. V. Drosdov, "Application of Acoustic Emission Technique in the Studies of Structural Ceramics Strength under Conditions of Mechanical and Thermal Loading," *Proc. Int. Conf. Nondestr. Test., 10th,* 345–52 (1982).

[19]P. F. Becher, "Subcritical Crack Growth in Partially Stabilized ZrO_2 (MgO)," *J. Mater. Sci.*, **21**, 297–300 (1986). □